Effect of Substrate Surfaces for Crystal Growth of a Photochromic Diarylethene by Sublimation

Effect of Substrate Surface for Crystal Growth of a Photochromic Diarylethene by Sublimation

Mami Isobe,[1,2] Daichi Kitagawa,[1,2] and Seiya Kobatake[1,2]*

[1]Department of Chemistry and Bioengineering, Graduate School of Engineering Osaka Metropolitan University, 3-3-138 Sugimoto, Sumiyoshi-ku, Osaka 558-8585, Japan

[2]Department of Applied Chemistry and Bioengineering, Graduate School of Engineering Osaka City University, 3-3-138 Sugimoto, Sumiyoshi-ku, Osaka 558-8585, Japan

KEYWORDS. Photochromism; Diarylethene; Sublimation; Crystal morphology; Heteroepitaxy

ABSTRACT: The state of the substrate surface is one of the key factors in varying morphologies of crystals produced by sublimation method of some organic compounds. In this work, we succeeded in separately preparing different morphology of rodlike crystals of 1,2-bis(2,5-dimethyl-3-thienyl)perfluorocyclopentene (**1a**), which are classified into the hollow crystal and the feather-like crystal, by sublimation to glass substrates with the hydrophilic and hydrophobic surface, respectively. To clarify the crystal growth process on each surface of the glass substrate, we investigated miller indices of crystal faces attached to the substrate surface in the early stage of sublimation and crystal growth directions of these rodlike crystals from these crystal faces by X-ray diffraction measurements and polarizing microscopic observation. As a result, it was revealed that heterojunction between the crystal faces produced in the early and following stages of sublimation leads to two different crystal morphologies. Moreover, it was confirmed that the heterojunctions occur in a specific orientation between these crystal faces because the lattice points in these crystal faces are in good agreement. Finally, we have demonstrated photomechanical behaviors of the hollow and feather-like crystals.

INTRODUCTION

Photochromism is a reversible transformation reaction between two isomers having different absorption spectra, which is induced in one or both directions by irradiation with light of certain wavelengths. Among many photochromic compounds, diarylethene derivatives have thermal stability of both isomers, fatigue resistance, high coloration quantum yield, and rapid response.[1,2] Diarylethenes can undergo reversible photochromism even in the crystalline phase,[3–5] some of which also present a variety of characteristic photoinduced shape change in their crystalline phase under the irradiation of UV light.[6–19] Thus far, it has been shown that the direction and/or speed of photoinduced bending and twisting behaviors of their rodlike crystals are highly related to both crystal shapes and molecular arrangements. Therefore, it is important for diarylethene derivatives to have their morphology to be modified for the creation and control of their photomechanical properties.

Sublimation is one of the vapor phase crystal growth methods, through which high-purity crystals are obtained on a substrate from the deposition source. Especially in vapor phase epitaxy, the growth layers are yielded with the crystal axis of them aligned with that of the substrates. In homoepitaxy, the growth layers are made up of the same material as the substrate, while in heteroepitaxy the growth layers are of a different material than the substrate, and a distinct crystallographic relationship exists between the orientations of the substrates and the growth layers. For the epitaxial layer in the presence of lattice mismatch between the growth layer and the substrate, a lattice mismatch ratio is commonly defined as the relative difference between the in-plane lattice constants of the growth layer and substrate.[20–22] The small lattice mismatch ratio means that the lattice points of the growth layer and the substrate are in good agreement. Some studies have estimated the lattice mismatch ratio of crystalline devices having electric and optical properties using various microscopic observation techniques in the vapor epitaxial growth process.[23–27]

The macroscopic and microscopic effects of the substrate surface on the molecular adsorption and nucleation phenomenon are essential in the vapor phase crystal growth process. Examples of the crystal growth methods by such microscopic effects of the substrate surface include van der Waals epitaxy, defined by Koma *et al.*[28–30] On the other hand, wettability is the macroscopic surface property that can be characterized by measuring the contact angle of water on solid surfaces. Some studies showed that the wettability can change crystal growth directions on the substrate and affects the crystal growth system for the organic compounds. Ikeda *et al.* reported the difference in the in-plane crystal orientation on the glass substrate with different wettability in the graphoepitaxy of *α*-sexithiophene.[31] Wang *et al.* showed that hydrophobic substrate is one of the key factors to affect the Nacre crystal growth system.[32,33] As mentioned above, it is likely that the surface wettability has some influence on the produced crystal morphology. Thus, it is required to figure out the crystal growth mechanism for each substrate surface with different wettability through an investigation of the process where the crystal morphologies are formed.

1,2-Bis(2,5-dimethyl-3-thienyl)perfluorocyclopentene (**1a**) (Figure 1) is one of the diarylethene derivatives exhibiting photochromism in the crystalline phase.[34] Most of the diarylethene crystals show the photomechanical effect

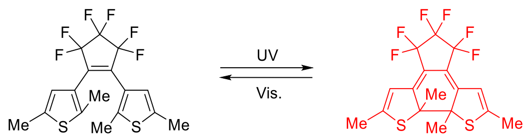

1a 1b

Figure 1. Photochromic reaction of **1a**.

associated with photochromism, but platelike crystals of **1a** yielded by recrystallization did not show any photomechanical behavior because only large size crystals are available by recrystallization. Platelike crystals of **1a** have rhombus- and rectangular-shaped faces, whose miller indices have been identified by single-crystal X-ray crystallographic analysis as $(01\bar{1})$ and $(100)/(1\bar{1}\bar{1})$, respectively.[34] These faces can be distinguished by observing the absorption anisotropy of polarized absorption spectrum of the photogenerated closed-ring form. Crystals suitable for photomechanical materials such as photoinduced bending are rodlike crystals, and research on methods for fabricating such crystals is indispensable.

In this study, we have focused on the effects of the substrate surface on crystal growth and morphology of **1a** obtained in the vapor phase crystal growth process, the objective of which was to find key factors related to sublimation conditions for separately preparing the crystal morphology of rodlike crystal of **1a**. To date, the vapor crystal growth process and mechanism of a photochromic diarylethene have not yet been explored. The knowledge obtained in this fundamental study will pave the way for controlling the crystal morphology of organic compounds by sublimation conditions.

EXPERIMENTAL SECTION

General. Solvents used were spectroscopic grade and purified by distillation before use. The polarized absorption spectra in the single crystalline phase were measured using a Nikon ECLIPSE E600POL polarizing optical microscope equipped with a Hamamatsu PMA-11 photonic multichannel analyzer as the photodetector and a super high-pressure mercury lamp (100 W) attached a UV-1A filter (365 nm light) as the light source. Visible light irradiation was carried out using a halogen lamp (100 W). Photomechanical behavior of crystals was observed using a Keyence VHX-500 digital microscope. UV irradiation was performed using a Keyence UV-LED UV-400/UV-50H (365 nm light). Visible light irradiation was carried out using a halogen lamp (100 W).

Cleaning the surface of the glass substrate. The glass substrate was immersed in a mixed solvent of methanol and hydrochloric acid (1:1) for 30 min, thoroughly washed with distilled water, dried under reduced pressure, then immersed in concentrated sulfuric acid for 24 h, thoroughly washed with boiling distilled water, then vacuum dried. The wettability of the surface of the prepared glass substrate was confirmed by measuring contact angles (θ) of 1 µL of the water drop on it (θ = 8°). The clean glass plate was used as a substrate with the hydrophilic surface.

Preparation of a glass substrate with hydrophobic surface by treating with a silane coupling agent. The glass substrate was cleaned as described above and was treated with *n*-hexyltrimethoxysilane (*n*-HTMS) by the wet method as follows: The water/ethanol solution was adjusted to about pH 3.3 using acetic acid and stirred for 10 min at 25 °C. Then, *n*-HTMS (2 wt% relative to the water/ethanol solution) was added to the stirred mixture and stirred subsequently for 5 min. The preprocessed glass substrate was soaked in the mixture for 2 min. After that, the substrate was rinsed with ethanol and dried in a vacuum at 110 °C for 5 min. The contact angle on the hydrophobic surface of the prepared glass substrate was 102°.

Setups and experimental conditions of sublimation method. To adjust humidity conditions in the sublimation system, we covered the whole of the sublimation apparatus with a dry cover equipped with a thermometer and a hygrometer (AS ONE NDC-2). Before starting sublimation, we adjusted relative humidity inside the dry cover to 20, 30, 40, 50, or 60%. When adjusting the humidity to 20, 30, or 40%, a hotplate and a beaker containing dry silica gel were set inside the dry cover. When adjusting the humidity to 50 or 60%, the hotplate and a beaker containing water were set inside the dry cover. The humidity control circuit in the case of the humidity of 50 or 60% was not used. After the humidity reaches equilibrium, the glass petri dish (height: 15 mm, inner diameter: 32 mm) containing powder crystals of **1a**, covered with the hydrophilic or hydrophobic glass substrate was put on the hotplate. Then, the 200 mL beaker containing ice water on the glass substrate was set, and the hotplate was heated to 100 °C. During sublimation for 2 h, we recorded the temperature and humidity inside the dry cover every 5 minutes and replenished the ice water every 30 min.

RESULTS AND DISCUSSION

Crystal morphology of rodlike crystals obtained by sublimation method. When powder crystals of **1a** were heated from 30 °C to 100 °C on a hot plate under atmospheric pressure using the sublimation apparatus shown in Figure 2a, rodlike crystals with several millimeters in length were densely produced on a glass substrate. These rodlike crystals were classified into two crystal morphologies by observing them with optical microscopy. One has a hollow in the direction along with its crystal-long axis and was named 'hollow crystal'. The other is flattened and has a sharp tip and was named 'feather-like crystal'. To get knowledge of crystal structures and directions of crystal-long axis for two kinds of the obtained rodlike crystal, X-ray diffraction (XRD) measurement for these crystals was performed by irradiating X-ray to the faces of these crystals. According to XRD patterns of each rodlike crystal and the pattern calculated from single-crystal X-ray crystallographic analysis data of **1a**[34] (Figure 2b), a sharp, strong-intensity peak of $(100)/(1\bar{1}\bar{1})$ plane and weak-intensity peak of $(200)/(2\bar{2}\bar{2})$ were observed for the hollow crystal, and a sharp, strong-intensity peak of $(01\bar{1})$ plane and weak-intensity peak of $(02\bar{2})$ were observed for the feather-like crystals. These indicate that the hollow and feather-like crystals have $(100)/(1\bar{1}\bar{1})$ plane and $(01\bar{1})$ plane, respectively, for the well-developed faces. In addition, the hollow crystal has a rhombus-shaped cross-section, angles of which are 75° and 105°. This indicates that the cross-section corresponds to the $(01\bar{1})$ plane as shown in Figure 2c. Also, the feather-like crystal has a parallelogram with angles of 37.5° and 142.5°. The direction of the crystal-long axis of the feather-like crystal was classified into A and B in Figure 2c, which depend on angles between its crystal growth direction (red two-way arrows) and the substrate surface. In A, crystal growth occurs vertically from the glass surface. On the other hand, in B, crystal growth occurs at an angle of 52.5° from the glass surface, as shown in Figure 2d. In summary, the hollow crystal and the feather-like crystal have the same crystal structure of **1a** while their crystal growth directions are different from each other.

Sublimation condition to separately prepare crystals with different morphologies. According to the analysis of crystal morphologies for each rodlike crystal in the previous section, they have different crystal growth directions, which means they have different crystal growth rates. To investigate the crystal growth rate of each rodlike crystal, we observed the process of sublimation of **1a** under the same condition as before by shooting a movie in the vicinity of the substrate surface using a digital microscope as shown in Figure 3a. Determining crystal growth rates of each rodlike crystal from the time-lapse photograph of the sublimation process, it was found that a hollow crystal grew at 0.2 μm s^{-1} while a feather-like crystal grew at 2.0 μm s^{-1} in the direction of the crystal-long axis of each rodlike crystal, as shown in Figure 3b,c. This result indicates that two kinds of rodlike crystals can be prepared separately by taking out the substrate at different times. In addition, these photographs show that a hollow crystal began to grow 10 min after start heating while a feather-like crystal began to grow 5 min after start heating. During such time frames, nucleation of crystals seems to proceed on the substrate surface, which takes different times, depending on miller indices of crystal faces attached on the substrate surface in the early stage of the sublimation process.

It is important to fabricate the hollow crystals and the feather-like crystals separately. Here, we compared the formation of crystal depending on the surface condition of two types of substrates, a cleaned glass substrate and an alkyl silane modified substrate. First, crystal growth due to differences in humidity was examined using a dry cover to confirm the effect of atmospheric humidity under sublimation conditions. The difference in morphology of the crystals produced at 20% to 60% humidity is shown in Figure S1 and Table S1. The result indicates that the wettability of the substrate surface has an influence on the nucleation process of **1a** under that experimental condition, which leads to the generation of different crystal morphologies of each rodlike crystal on the substrate surface with different wettability. It was found that at 40% humidity, hollow crystals and feather-like crystals were produced independently on the hydrophilic and the hydrophobic substrates, respectively. As shown in Figure 4a,

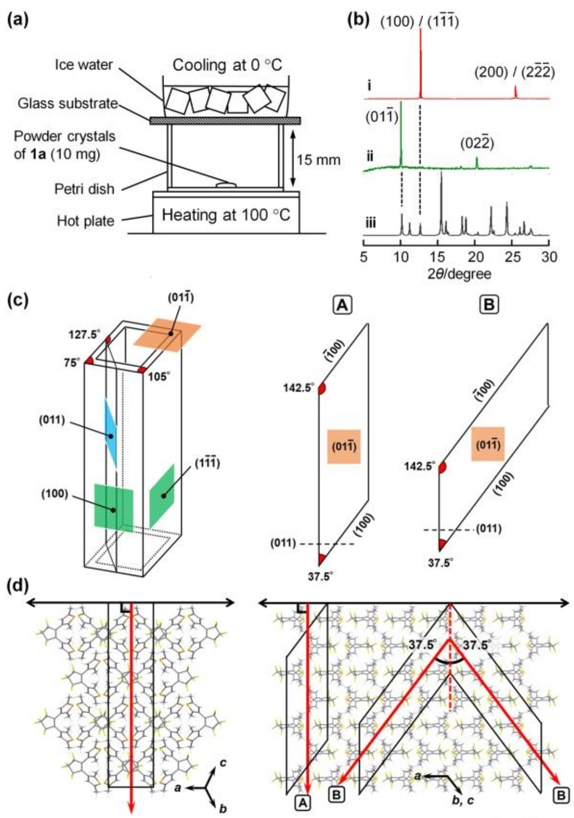

Figure 2. Sublimation method for preparing rodlike crystals of **1a** and characterization of the crystals: (a) Setup of the sublimation method, (b) XRD of (i) feather-like crystal, (ii) hollow crystal having a complete rhombus-shaped hollow structure, and (iii) pattern calculated from single-crystal X-ray crystallographic analysis data powder crystal, (c) crystal shapes identified with miller indices for the feather-like crystal and hollow crystal of **1a** (triclinic, $P\bar{1}$, a = 8.833 Å, b =11.178 Å, c =11.431 Å, α = 100.588°, β = 112.708°, γ = 113.218°)[34], (d) the packing diagrams of **1a**. The black and red arrows in (d) indicate glass surface and crystal growth directions from the glass surface, respectively.

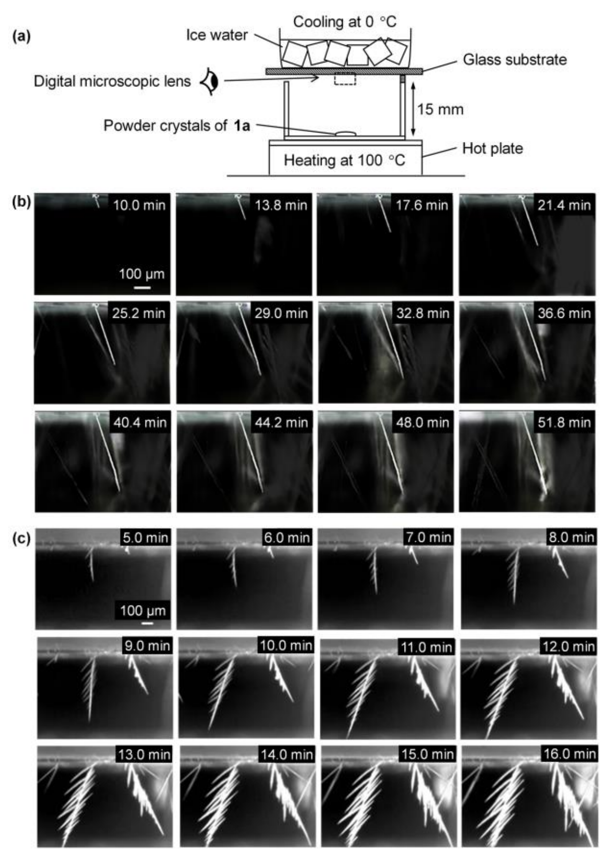

Figure 3. (a) Setup for observation in a sublimation process of **1a** and photographs during the growth process of (b) a hollow crystal and (c) a feather-like crystal. The figure in the upper-right corner of each photograph indicates the time elapsed from the starting of the sublimation.

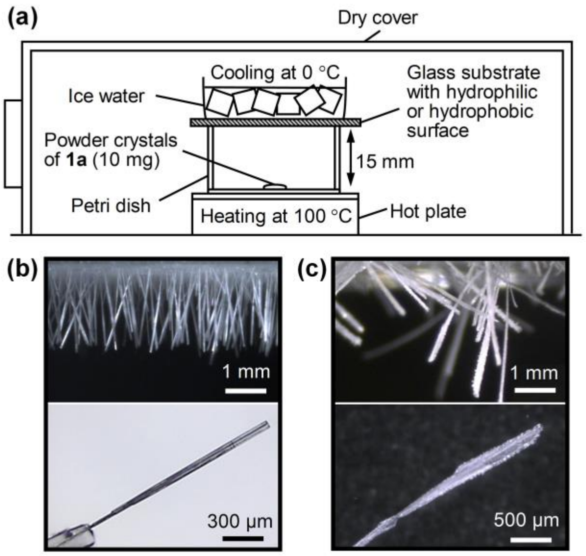

Figure 4. Sublimation method for preparing rodlike crystals of **1a** using glass substrates with different wettability: (a) Setup of the sublimation method, (b, c) crystal morphologies of rodlike crystals grown on glass substrates with (b) hydrophilic and (c) hydrophobic surfaces, respectively. Rodlike crystals having each crystal morphology were prepared by sublimation for 2 h under 40% relative humidity.

relative humidity was kept 40% for 10 min after heating with a hygrometer attached to the dry cover. After 2 h of heating, hollow crystals have been grown on the hydrophilic surface of the glass substrate as shown in Figure 4b, while feather-like crystals have been grown on the hydrophobic surface of it as shown in Figure 4c. Under sublimation conditions adjusted to a wide range of relative humidity, it was also confirmed the hollow crystal and the feather-like crystal grew on the substrate surface with hydrophilic (Figure 4b) and hydrophobic (Figure 4c), respectively.

X-ray diffraction analysis of crystals on substrate surfaces with different wettability. To investigate changes in miller indices of crystals obtained on the substrate surface with different wettability during sublimation, we performed XRD measurement of the crystals obtained on each substrate surface. Figure 5a shows XRD patterns of crystal **1a** obtained from the hydrophilic substrate surfaces by heating for (i) 3 min at 80 °C, (ii) 10 min at 100 °C, and (iii) 120 min at 100 °C. The crystal faces of (011) plane are attached to the substrate surface in the early stage of sublimation, and then, the area of the substrate surface gets gradually occupied with more crystal faces of (01$\bar{1}$) plane than those of (011) plane. In the final stage of the sublimation, the crystal faces of (01$\bar{1}$) plane spread on the most area of the substrate surface. It indicates that thin film composed of crystal face of (011) is formed on the surface of the hydrophilic glass substrate in the early stage of sublimation to follow that the thin film is gradually covered with crystal face of (01$\bar{1}$).

Figure 5b shows XRD patterns of crystals obtained from the hydrophobic substrate surfaces of (i) 2 min at 65 °C, (ii) 5 min at 95 °C, and (iii) 120 min at 100 °C after start heating. According to them, in the early stage of sublimation, crystal faces of (01$\bar{1}$) plane attached to the substrate surface, and then, the area occupied with more crystal faces of (011) plane than those of (01$\bar{1}$) plane, and finally, crystal faces of (011) plane spread on the most area of the substrate surface. Observing the crystals generated on the hydrophobic substrate surface of each time, micro-sized crystals were generated sparsely a few

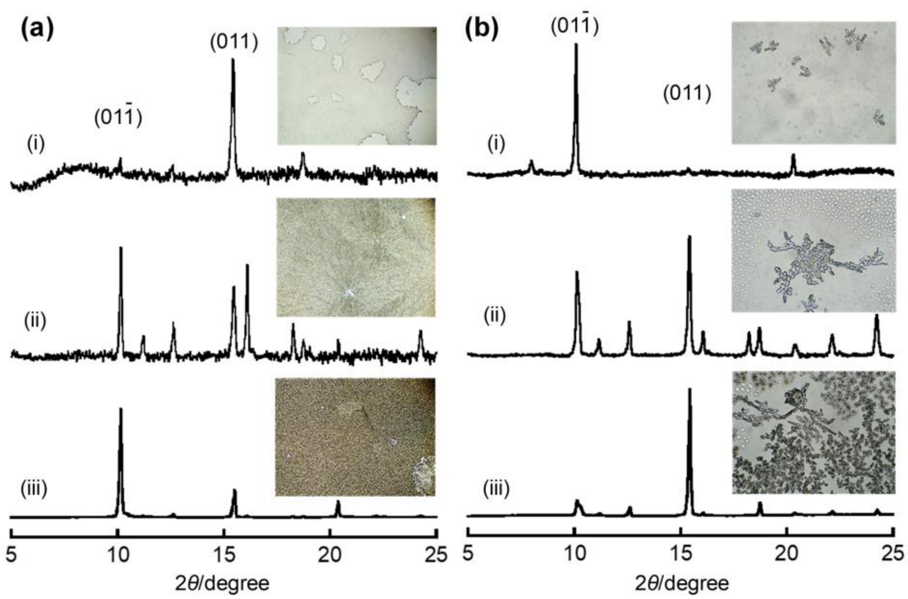

Figure 5. XRD patterns and photographs for sublimation (a) on the hydrophilic substrate surface by heating for (i) 3 min at 80 °C, (ii) 10 min at 100 °C, and (iii) 120 min at 100 °C and (b) on the hydrophobic substrate surface by heating for (i) 2 min heating at 65 °C, (ii) 5 min heating at 95 °C, and (iii) 120 min heating at 100 °C.

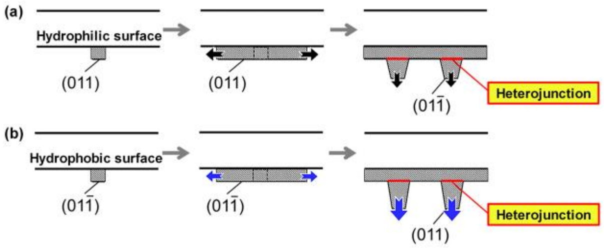

Figure 6. Crystal growth mechanism of vapor phase crystal growth of **1a** on a glass substrate with (a) the hydrophilic and (b) hydrophobic surfaces. Red lines indicate heterojunction.

Table 1. Heterojunction patterns between $(01\bar{1})$ and (011) planes.

Pattern	Distance[a]/Å	Number of matching lattice points[b]
I	0.24	6
II	0.53	4

[a]Distance between closest lattice points. [b]Number of matching lattice points included in the shaded area in Figure 7.

minutes after starting sublimation. Then, they grew in dendrite crystals with a lot of droplets of **1a** surrounding themselves, and many dendrite crystals were produced on the entire area of the hydrophobic substrate surface after 120 min heating.

To summarize, the crystal growth mechanism on a glass substrate with the hydrophilic and hydrophobic surfaces are shown in Figure 6. In the case of the hydrophilic surface, crystal faces of the (011) plane attach to the substrate surface and a polycrystalline thin film having (011) plane on their surface are formed at an early stage of sublimation. Then, crystal faces of $(01\bar{1})$ plane join to (011) plane on the surface of the polycrystalline thin film through heterojunction. In contrast, on the hydrophobic surface, crystal faces having $(01\bar{1})$ plane attach on the substrate surface and some micro-sized crystals having $(01\bar{1})$ plane grows in the dendrite crystals in the early stage of sublimation. After that, crystal faces of (011) plane join to $(01\bar{1})$ plane on the surface of the dendrite crystals through the heterojunction. That is why the hollow and the feather-like crystals are produced on the hydrophilic and the hydrophobic substrate, respectively.

Heteroepitaxial growth depending on lattice mismatch. The heterojunction between $(01\bar{1})$ and (011) planes induced on both the hydrophilic and hydrophobic surfaces during the sublimation process of **1a** can be explained in more detail from the point of view of lattice mismatch (Figure 7). The method of determining some heterojunction patterns which are more likely to generate by calculating the lattice mismatch ratio between $(01\bar{1})$ and (011) planes is as follows: Coplanar lattice points included in molecular arrangements of **1a** are presented as large orange and blue dots when viewed from $(01\bar{1})$ and (011) planes, respectively. These coplanar lattice points on the $(01\bar{1})$ and

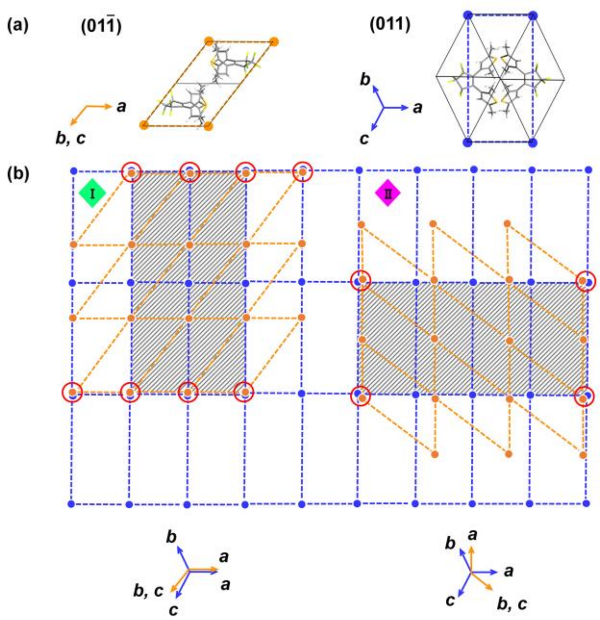

Figure 7. Lattice mismatch between $(01\bar{1})$ and (011) planes on the different heterojunction pattern. Orange and blue dots in (a) represent lattice points within the cross-section of unit cell of **1a**, which are parallel to $(01\bar{1})$ and (011) planes, respectively. Each cross-section for $(01\bar{1})$ and (011) planes is surrounded by dashed orange and blue lines, respectively. Heterojunction patterns, I and II, in (b) are combinations of each arrangement of the cross-sections for $(01\bar{1})$ and (011) planes where the most lattice points match. Red circles represent a good match between lattice points of $(01\bar{1})$ and (011) planes.

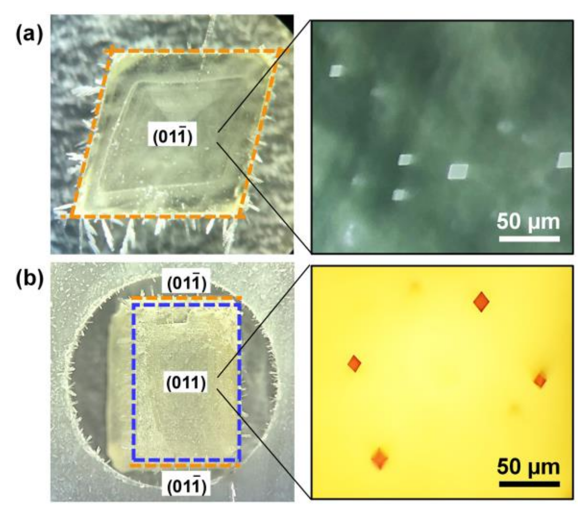

Figure 8. Photographs of sublimation on (a) $(01\bar{1})$ and (b) (011) surfaces of the platelike single crystal of **1a** in the early stage of the sublimation process. The rodlike crystals in (b) were dyed red by UV irradiation to make the crystals clear.

(011) planes are connected by orange and blue dashed lines, respectively. When arranging the lattice plane of $(01\bar{1})$ presented as the orange square and that of (011) plane presented as the blue square in a certain direction, some of the arrangements was found to be the heterojunction patterns with lattice point matches. One is in a case of *a*-axis for these lattice planes of $(01\bar{1})$ and (011) planes aligned (pattern I), and another is obtained when rotating the lattice plane of $(01\bar{1})$ plane in pattern I by 90° in a counterclockwise direction (pattern II). We affirmed how far these lattice planes of $(01\bar{1})$ and (011) planes are matched by calculating the distance between the closest lattice points of $(01\bar{1})$ and (011) planes. Table 1 shows the distance between closest lattice points (*D*) for each patten I and II. Very small values of *D* are calculated for both heterojunction patterns, so, we determined pattern I and II as the heterojunction patterns which are more likely to generate.

Moreover, we confirmed that the two heterojunction patterns having the less value of *D* are actually easier to be formed. We sublimated powder crystals of **1a** to the surface of the bulk single crystal of **1a**, identified with $(01\bar{1})$ and (011) planes, and observed directions of tip of the hollow crystals generated on these surfaces of the bulk single crystal of **1a**. As shown in Figure 8a, many rhombus shaped cross-sections of the hollow crystals, all of which are $(01\bar{1})$ plane, have grown in the same direction through homoepitaxial growth on the surface of the $(01\bar{1})$ plane of the bulk crystal of **1a** under relatively low-humidity conditions. On the other hand, as shown in Figure 8b, many hollow crystals were produced in the same direction through heteroepitaxial growth on the (011) plane of the bulk crystal of **1a** under relatively high-humidity conditions. Such crystal growth direction of them stems from the crystal growth process through heterojunction pattern I due to a good match of the lattice points of $(01\bar{1})$ and (011) planes.

Photomechanical behavior of rodlike crystals. We examined photomechanical behaviors of the hollow crystal and the feather-like crystal. As shown in Figure 9a, when the hollow crystal was irradiated with UV light (365 nm light, 94 mW cm^{-1}) to the side face for 3 s, it bent toward the light source. After the irradiation with UV light, it returned to the initial position under irradiation with visible light. On the other hand, the feather-like crystal irradiated with UV light (365 nm light, 375 mW cm^{-1}) to the side face for 5 s bent against the light source (Figure 9a). When irradiated with visible light following the bending behavior, however, it did not go back completely where it started. It indicates that the feather-like crystal produces strains in itself during photoinduced bending behavior and reduces crystallinity.

Conclusions. We succeeded in separately preparing the rodlike crystals of **1a** with different morphology on each surface of the glass substrate having different wettability under the controlled humidity conditions. On the hydrophilic substrate surface, a polycrystalline thin film with a surface corresponding to (011) plane is first formed, and then the hollow crystals with the $(01\bar{1})$ cross section grow through heterojunction. On the hydrophobic substrate surface, however, dendrites with a surface corresponding to $(01\bar{1})$ plane are generated, and then the feather-like crystals with (011) cross section grow through heterojunction. The difference in crystal growth mechanism between the hollow crystals and the feather-like crystals was clarified by the XRD measurement and polarization microscopic observation for the crystals produced on each of the substrate surfaces after sublimation for several minutes and

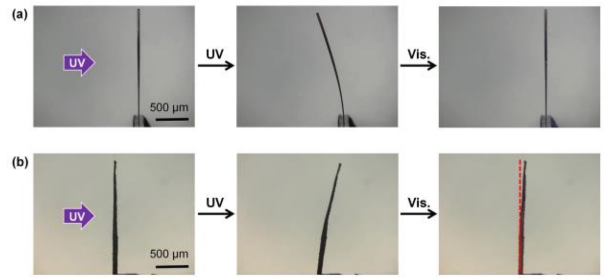

Figure 9. Photoinduced bending behaviors of (a) the hollow crystal and (b) the feather-like crystal under irradiation with UV light to the left side of each rodlike crystal for 3 s and 5 s, respectively. The hollow crystal returns to the initial position while the feather-like crystal does not completely return to the initial stage under irradiation with visible light. Red dashed line shows the initial position of the feather-like crystal.

2 h, respectively. The close distance between closest lattice points of $(01\bar{1})$ and (011) planes and a larger number of matching lattice points in the certain area contribute to good lattice matching between thin films or dendrites and cross-sections of each rodlike crystal through certain kinds of heterojunction pattern. Moreover, it was confirmed that the hollow crystals are produced through heteroepitaxial growth on (011) plane of the bulk crystal of **1a**. Finally, when irradiated with UV light to the side faces of each rodlike crystal, the hollow crystal bends toward the light source and returns to the initial state under irradiation with visible light. The feather-like crystal bends against the light source with the generation of strain in itself.

ASSOCIATED CONTENT

SUPPORTING INFORMATION

The Supporting Information is available free of charge at https://pubs.acs.org/doi/10.1021/acs.cgd.*******.

Detailed experimental data for Crystal morphology of rod crystals of **1a** generated by sublimation under conditions of different relative humidity (PDF)

AUTHOR INFORMATION

Corresponding Author

Seiya Kobatake − *Department of Chemistry and Bioengineering, Graduate School of Engineering, Osaka Metropolitan University, 3-3-138 Sugimoto, Sumiyoshi-ku, Osaka 558-8585, Japan; Department of Applied Chemistry and Bioengineering, Graduate School of Engineering, Osaka City University, 3-3-138 Sugimoto, Sumiyoshi-ku, Osaka 558-8585, Japan*; orcid.org/0000-0002-1526-4629; Email: kobatake@omu.ac.jp

Authors

Mami Isobe − *Department of Chemistry and Bioengineering, Graduate School of Engineering, Osaka Metropolitan University, 3-3-138 Sugimoto, Sumiyoshi-ku, Osaka 558-8585, Japan; Department of Applied Chemistry and Bioengineering, Graduate School of Engineering, Osaka City University, 3-3-138 Sugimoto, Sumiyoshi-ku, Osaka 558-8585, Japan*

Daichi Kitagawa − *Department of Chemistry and Bioengineering, Graduate School of Engineering, Osaka Metropolitan University, 3-3-138 Sugimoto, Sumiyoshi-ku, Osaka 558-8585, Japan; Department of Applied Chemistry and Bioengineering, Graduate School of Engineering, Osaka City University, 3-3-138 Sugimoto, Sumiyoshi-ku, Osaka 558-8585, Japan*; orcid.org/0000-0002-1994-3047

Author Contributions

The manuscript was written through the contributions of all authors. All authors have approved the final version of the manuscript.

Notes

The authors declare no competing financial interest.

ACKNOWLEDGMENTS

This work was partly supported by JSPS KAKENHI grants 21K14603 in Grant-in-Aid for Early-Career Scientists for D. K. and 21H02016 in Grant-in-Aid for Scientific Research (B) for S. K.

REFERENCES

(1) Irie, M.; Fukaminato, T.; Matsuda, K.; Kobatake, S. Photochromism of Diarylethene Molecules and Crystals: Memories, Switches, and Actuators. *Chem. Rev.* **2014**, *114*, 12174−12277.

(2) Irie, M. *Diarylethene Molecular Photoswitches: Concepts and Functionalities*, John Wiley & Sons, 2021.

(3) Kobatake, S.; Irie, M. Single-Crystalline Photochromism of Diarylethenes. *Bull. Chem. Soc. Jpn.* **2004**, *77*, 195−210.

(4) Irie, M.; Kobatake, S.; Horichi, M. Reversible Surface Morphology Changes of a Photochromic Diarylethene Single Crystal by Photoirradiation. *Science* **2001**, *291*, 1769−1772.

(5) Shibata, K.; Muto, K.; Kobatake, S.; Irie, M. Photocyclization/Cycloreversion Quantum Yields of Diarylethenes in Single Crystals. *J. Phys. Chem. A* **2002**, *106*, 209−214.

(6) Kobatake, S.; Takami, S.; Muto, H.; Ishikawa, T.; Irie, M. Rapid and Reversible Shape Changes of Molecular Crystals on Photoirradiation. *Nature* **2007**, *446*, 778−781.

(7) Morimoto, M.; Irie, M. A Diarylethene Cocrystal that Converts Light into Mechanical Work. *J. Am. Chem. Soc*. **2010**, *132*, 14172−14178.

(8) Terao, F.; Morimoto, M.; Irie, M. Light-Driven Molecular-Crystal Actuators: Rapid and Reversible Bending of Rodlike Mixed Crystals of Diarylethene Derivatives. *Angew. Chem. Int. Ed*. **2012**, *51*, 901−904.

(9) Irie, M. Photochromism and Molecular Mechanical Devices. *Bull. Chem. Soc. Jpn*. **2008**, *81*, 917−926.

(10) Kitagawa, D.; Nishi, H.; Kobatake, S. Photoinduced Twisting of a Photochromic Diarylethene Crystal. *Angew. Chem. Int. Ed.* **2013**, *52*, 9320−9322.

(11) Kitagawa, D.; Tsujioka, H.; Tong, F.; Dong, X.; Bardeen, C. J.; Kobatake, S. Control of Photomechanical Crystal Twisting by Illumination Direction. *J. Am. Chem. Soc*. **2018**, *140*, 4208−4212.

(12) Kitagawa, D.; Kawasaki, K.; Tanaka, R; Kobatake, S. Mechanical Behavior of Molecular Crystals Induced by Combination of Photochromic Reaction and Reversible Single-Crystal-to-Single-Crystal Phase Transition. *Chem. Mater.* **2017**, *29*, 7524−7532.

(13) Iwaihara, C.; Kitagawa, D.; Kobatake, S. Polymorphic Crystallization and Thermodynamic Phase Transition between the Polymorphs of a Photochromic Diarylethene. *Cryst. Growth Des.* **2015**, *15*, 2017−2023.

(14) Hirano, A.; Kitagawa, D.; Kobatake, S. Photomechanical Bending Behavior of Photochromic Diarylethene Crystals Induced under Polarized Light. *CrystEngComm* **2019**, *21*, 2495−2051.

(15) Kitagawa, D.; Okuyama, T.; Tanaka, R.; Kobatake, S. Photoinduced Rapid and Explosive Fragmentation of Diarylethene Crystals Having Urethane Bonding. *Chem. Mater.* **2016**, *28*, 4889−4892.

(16) Tamaoki, M.; Kitagawa, D.; Kobatake, S. Light-Driven Rapid Peeling of Photochromic Diarylethene Single Crystals. *Cryst. Growth Des.* **2021**, *21*, 3093−3099.

(17) Nishimura, R.; Hyodo, K.; Mayama, H.; Yokojima, S.; Nakamura, S.; Uchida, K. Dual Wettability on Diarylethene Microcrystalline Surface Mimicking a Termite Wing. *Commun. Chem*. **2019**, *2*, 90.

(18) Hatano, E.; Morimoto, M.; Imai, T.; Hyodo, K.; Fujimoto, A.; Nishimura, A.; Sekine, A.; Yasuda, N.; Yokojima, S.; Nakamura, S.; Uchida, K. Photosalient Phenomena that Mimic Impatiens Are Observed in Hollow Crystals of Diarylethene with a Perfluorocyclohexene Ring. *Angew. Chem. Int. Ed.* **2017**, *56*, 12576−12580.

(19) Fujimoto, A.; Fujinaga, N.; Nishimura, R.; Hatano, E.; Kono, L.; Nagai, A.; Sekine, A.; Hattori, Y.; Kojima, Y.; Yasuda, N.; Morimoto, M.; Yokojima, S.; Nakamura, S.; Feringa, B. L.; Uchida, K. Photoinduced Swing of a Diarylethene Thin Broad Sword Shaped Crystal: A Study on the Detailed Mechanism. *Chem. Sci*. **2020**, *11*, 12307−12315.

(20) Sakurai, M.; Tada, H.; Saiki, K.; Koma, A.; Funasaka, H.; Kishimoto, Y. Epitaxial Growth of C_{60} and C_{70} Films on GaSe (0001) and MoS_2 (0001) Surfaces. *Chem. Phys. Lett.* **1993**, *208*, 425−430.

(21) Nakayama, Y.; Mizuno, Y.; Hosokai, T.; Koganezawa, T.; Tsuruta, R.; Hinderhofer, A.; Gerlach, A.; Broch, K.; Belova, V.; Frank, H.; Yamamoto, M.; Niederhausen, J.; Glowatzki, H.; Rabe, J. P.; Koch, N.; Ishii, H.; Schreiber, F.; Ueno, N. Epitaxial Growth of an Organic p-n Heterojunction: C_{60} on Single-Crystal Pentacene. *ACS Appl. Mater. Interfaces* **2016**, *8*, 13499−13505.

(22) Takahashi, K.; Izawa, S.; Ohtsuka, N.; Izumiseki, A.; Tsuruta, R.; Takeuchi, R.; Gunjo, Y.; Nakanishi, Y.; Mase, K.; Koganezawa, T.; Momiyama, N.; Hiramoto, M.; Nakayama, Y. Quasi-Homoepitaxial Junction of Organic Semiconductors: A Structurally Seamless but Electronically Abrupt Interface between Rubrene and Bis(trifluoromethyl)dimethylrubrene. *J. Phys. Chem. Lett*. **2021**, *12*, 11430−11437.

(23) Yamaguchi, H.; Homma, Y. Imaging of Layer by Layer Growth Processes during Molecular Beam Epitaxy of GaAs on (111)A Substrates by Scanning Electron Microscopy. *Appl. Phys. Lett*. **1998**, *73*, 3079−3081.

(24) Hassan, J.; Bergman, J. P.; Henry, A.; Janzén, E. On-Axis Homoepitaxial Growth on Si-face 4H–SiC Substrates. *J. Crystal Growth* **2008**, *310*, 4424−4429.

(25) Lavini, F.; Cellini1, F.; Rejhon, M.; Kunc, J.; Berger, C.; de Heer, W.; Riedo, E. Atomic Force Microscopy Phase Imaging of Epitaxial Graphene Films. *J. Phys. Mater*. **2020**, *3*, 024005.

(26) Nylund, I. E.; Raeder, T. M.; Vullum, P. E.; Grande, T. Epitaxial (100), (110), and (111) $BaTiO_3$ Films on $SrTiO_3$ Substrates-A Transmission Electron Microscopy Study. *J. Appl. Phys*. **2021**, *129*, 095304.

(27) Guo, H.; Zhang, J. Scanning Probe Microscopy (SPM) of Epitaxial Oxide Thin Films. In *Epitaxial Growth of Complex Metal Oxides*; Koster, G.; Huijben, M.; Rijnders, G. Eds.; Woodhead Publishing: Cambridge, 2015; pp. 295−328.

(28) Koma, A.; Sunouchi, K.; Miyajima, T. Fabrication and Characterization of Heterostructures with Subnanometer Thickness *Microelectron. Eng.* **1984**, *2*, 129−136.

(29) Koma, A.; Sunouchi, K.; Miyajima, T. Fabrication of Ultrathin Heterostructures with van der Waals Epitaxy. *J. Vac. Sci. Technol. B* **1985**, *3*, 724.

(30) Koma, A. Van der Waals Epitaxy-A New Epitaxial Growth Method for a Highly Lattice-Mismatched System. *Thin Solid Films*. **1992**, *216*, 72−76.

(31) Ikeda, S.; Saiki, K.; Wada, Y.; Inaba, K.; Ito, Y.; Kikuchi, H.; Terashima, K.; Shimada, T. Graphoepitaxy of Sexithiophene and Orientation Control by Surface Treatment. *J. Appl. Phys.* **2008**, *103*, 084313.

(32) Wang, R.; Gao, R.; Feng, X.; Zhang, G. Nacre Crystal Growth as a Paradigm of Island Growth Mode: Hydrophobic Substrate is One of the Keys to the Biomineralization. *Mater. Express* **2020**, *10*, 762−769.

(33) Feng, X.; Gao, R.; Wang, R.; Zhang, G. Non-Classical Crystal Growth on a Hydrophobic Substrate. *CrystEngComm* **2020**, *22*, 3100−3105.
(34) Kobatake, S.; Yamada, T.; Uchida, K.; Kato, N.; Irie, M. Photochromism of 1,2-Bis(2,5-dimethyl-3-thienyl)perfluorocyclopentene in a Single Crystalline Phase. *J. Am. Chem. Soc.* **1999**, *121*, 2380−2386.

For Table of Contents Use Only

Effect of Substrate Surface for Crystal Growth of a Photochromic Diarylethene by Sublimation

Mami Isobe, Daichi Kitagawa, and Seiya Kobatake*

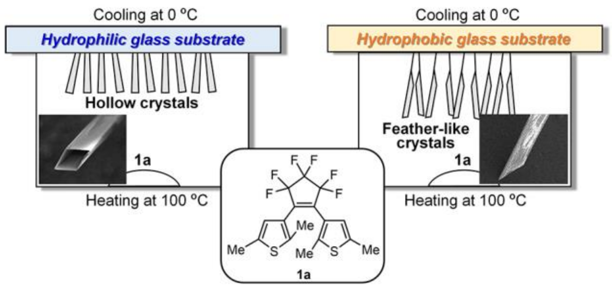

SYNOPSIS:

Sublimation of **1a** to glass substrates with hydrophilic and hydrophobic surfaces gives rodlike crystals of **1a** having different types of crystal morphologies, classified into the hollow crystal and the feather-like crystal, respectively.